Electronic Supplementary Material (ESI) for Journal of Materials Chemistry A.

Synergistic Interaction of Perovskite Oxides and N-doped Graphene in Versatile Electrocatalyst

Yunfei Bu,[a] *Haeseong Jang,*[b] *Ohhun Gwon,* [b] *Su Hwan Kim,*[b] *Se Hun Joo,*[b] *Gyutae Nam,*[b] *Seona Kim,*[b] *Yong Qin,*[d] *Qin Zhong,*[c] *Sang Kyu Kwak*, [b*] *Jaephil Cho,* [b*] *Guntae Kim* [b*]

[a] Jiangsu Collaborative Innovation Center of Atmospheric Environment and Equipment Technology (CICAEET), School of Environmental Science and Engineering, Nanjing University of Information Science and Technology. 210044, PR of China.

[b] Department of Energy Engineering, Ulsan National Initute of Science and Technology, Ulsan, 44919, South Korea.

[c] School of Chemical Engineering, Nanjing University of Science and Technology, Nanjing 210094, PR of China.

[d] School of Chemical Engineering, Changzhou University, Changzhou, 210000, PR of China.

Experimental Section

All the reagents used in the experiment were of analytical grade and used without further purification.

***Preparation of $(PrBa_{0.5}Sr_{0.5})_{0.95}Co_{1.5}Fe_{0.5}O_{5+\delta}$ (PBSCF) nanofibers**:*

The hollow nanofibers P-HF were prepared via an electrospinning technique. The stoichiometric amount of $Pr(NO_3)_3 \cdot 4H_2O$, $Ba(NO_3)_2$, $Sr(NO_3)_2$ $Fe(NO_3)_2 \cdot 6H_2O$ and $Co(NO_3)_2 \cdot 6H_2O$ were dissolved in *N,N*-dimethylformamide (DMF). Then Pluronic F127 was added to the solution. After all dissolve, polyacrylonitrile (PAN) was added to the solution Then, the mixture was stirred for 24 h under 80 ^oC controlled by hot plate to ensure dissolution of precursor materials. The as-prepared PBSCF precursor solution was loaded into a plastic syringe equipped with stainless steel needle electrically connected to the high voltage power supply. The distance between the needle tip and the collector was around 15 cm. After a voltage of 20 kV was applied, the fibers formed via the electrostatic forces and deposited on aluminum foil on the rotating metal drum. After electrospinning, the electrospun film was dried and then calcined at 900 ^oC for 2 h with the ramping rate 1 ^oC min^{-1}.

***Electrochemical measurements**:*

The electrochemical tests were carried out using a computer-controlled potentiostat (Biologic VMP3) with an RRDE-3A rotating disk electrode system. A platinum wire was used as the counter-electrode and an Hg/HgO (1 M NaOH filled) electrode as the reference electrode for ORR and OER. (The graphite rod (Alfa Aesar, 99.9995%) was used as the counter electrode for HER), while RRDE with various samples was served as working electrode. The catalyst membranes were prepared using a refined slurry coating technology. The mixtures of catalyst inks were prepared by physically mixing 20 mg catalyst powders with 0.1 mL of 5 wt% Nafion (Aldrich) solution and 0.9 mL of isopropyl alcohol solution, followed by ultrasonication the mixture for 0.5 h to form homogeneous catalysts inks. 5 μL of the catalysts ink was dropped onto a polished glassy carbon (GC) electrode of 4 mm diameter. Catalyst-coated GC electrodes with an area of 0.1256 cm^{-2} were then dried at room temperature for 1 h. The onset overpotential is determined by the potential when the plot

starts to deviate from the linear region. The electron transfer number and peroxide yield were calculated based on the following equations.

$$n = 4 \times \frac{I_d}{I_d + \frac{I_r}{N}} \quad (1)$$

$$\%(HO_2^-) = 200 \times \frac{\frac{I_r}{N}}{I_d + \frac{I_r}{N}} \quad (2)$$

where Id is disk current, Ir is ring current, and the collection efficiency (N) was determined to be 0.4 by using 10 mM $K_3[Fe(CN)_6]$.

The overall water splitting tests were performed in a two-electrode system with catalysts loaded on Carbon paper (mass loading: 1 mg cm^{-2}). Polarization curves were obtained using LSV with a scan rate of 5 mV s^{-1}.

Calculation details:

Spin-polarized density functional theory (DFT) calculations were carried out using the Vienna ab-initio simulation package (VASP)[1-2]. The generalized gradient approximation with the Perdew-Burke-Ernzerhof functional (GGA-PBE)[3] was employed for the exchange-correlation potential of electrons. The electron-ion interaction was described by the projector augmented-wave (PAW)[4] method. The energy cutoff for the plane-wave basis set was set to be 550 eV. The Hubbard U (*i.e.*, U_{eff} = 3.3 and 4.0 eV) correction[5-6] was employed for the Co and Fe 3*d* electrons, respectively. The van der Waals interactions were corrected with Grimme's D2 method[7]. The dipole correction was applied along *z*-direction in all calculations. The convergence criterion for the self-consistent field (SCF) calculations was set to be 10^{-6} eV. The atomic positions and lattice parameters were fully relaxed until the Hellmann-Feynman forces acting on ions were less than 0.01 eV/Å. The Brillouin zone was integrated

using 3 × 3 × 3 and 3 × 3 × 1 k-point meshes with Monkhorst-Pack scheme for bulk and surface systems, respectively. Bader charge analysis[8-10] was implemented to investigate the atomic charges.

Model systems

The bulk $PrBa_{0.5}Sr_{0.5}Co_{1.5}Fe_{0.5}O_6$ (PBSCF) double perovskite was constructed by changing two Ba and Co atoms to Sr and Fe atoms from 2 × 2 × 1 supercell of $PrBaSrCoFeO_6$ (PBSCF), respectively. The lattice parameters of the bulk system were determined as $a = b = 7.595$ Å, $c = 7.853$ Å, and $\alpha = \beta = \gamma = 90.00°$. A symmetric slab model of (001) surface consisting of 7 atomic layers was constructed with the vacuum slab of 25 Å to avoid interaction between adjacent periodic slabs along the *z*-axis (**Figure S12a**). Two atomic layers at the bottom were fixed during optimization to consider the bulk-like effect. Nextly, to investigate the effect of 3DNG on PBSCF surface, the zig-zag carbon nanoribbon with N-doped edges were constructed (**Figure S12b**). Note that the ~3 % of misfit strain on *x*-axis was applied to 3DNG to match the periodic boundary of (001) surface of PBSCF.

Preparation and assembly of a rechargeable Zn-air battery:

Figure S12 shows a digital photograph of the rechargeable Zn-air batteries. Zinc plate was used as the anode which separated by a nylon polymer membrane separator (Cell guard 3501 membrane) with the cathode and 6 M KOH electrolyte was filled between the cathode and anode, nickel mesh was used as current collector. The only difference between the primary and rechargeable Zn-air battery was 0.2M Zinc acetate should be added in 6M KOH as electrolyte for rechargeable one. The air cathodes were prepared by coating a mixture of PTFE binder (60 wt % PTFE emulsion in water, Sigma-Aldrich), activated charcoal (Darco G-60A, Sigma-Aldrich) and electro-catalyst (PBSCF-NG or Pt/C+IrO_2) in a ratio of 65:8:27, respectively. Commercial catalyst pristine air electrode was used for comparison. An assembled full-cell was performed at several discharge and charge currents.

Characterizations:

XRD. The powder materials were subjected to the X-ray diffraction analysis (XRD, D8 Advance, Bruker diffractometer with Cu Kα radiation). During the test, the scan rate was 1° min^{-1} and the 2θ range was ranging from 20 to 80°.

SEM. The microstructure was examined by scanning electron microscopy (Nova FE-SEM).

TEM. Transmission electron microscope analysis of various samples was performed using were obtained using a High Resolution-TEM (JEOL, JEM-2100F).

BET. The BET specific surface areas of various catalysts were measured by the N_2 adsorption/desorption method using an Autosorb Quantachrome 1MP apparatus.

Oxygen nonstoichiometric ratio. The initial oxygen content of the perovskite at room temperature was determined using iodometric titration method. 20 mg of powder was placed in an Erlenmeyer flask followed by adding a small amount of 2 M KI solution. Then, 3.5 M HCl was added to completely dissolve the powders. During this process, a stream of N_2 flow was used to blanket the solution. The clear solution was titrated with a 0.01 M $Na_2S_2O_3$ solution using starch as the indicator.

References for DFT calculation

1. G. Kresse and J. Furthmüller, *Phys. Rev. B*, 1996, **54**, 11169-11186.

2. G. Kresse and J. Furthmüller, *Comp. Mater. Sci.*, 1996, **6**, 15-50.

3. J. P. Perdew, K. Burke and M. Ernzerhof, *Phys. Rev. Lett.*, 1996, **77**, 3865-3868.

4. G. Kresse and D. Joubert, *Phys. Rev. B*, 1999, **59**, 1758-1775.

5. Lee, Y.-L., Kleis, J., Rossmeisl, J., Shao-Horn, Y. & Morgan, D., *Energ. Environ. Sci.*, 2011, **4**, 3966–3970.

6. Lee, Y. L., Kleis, J., Rossmeisl, J. & Morgan, D, *Phys. Rev. B*, 2009, **80**, 224101.

7. S. Grimme, *J. Comput. Chem.*, 2006, **27**, 1787-1799.

8. W. Tang, E. Sanville and G. Henkelman, *J. Phys.-Condens. Mat.*, 2009, **21**, 084204.

9. E. Sanville, S. D. Kenny, R. Smith and G. Henkelman, *J. Comput. Chem.*, 2007, **28**, 899-908.

10. G. Henkelman, A. Arnaldsson and H. Jonsson, *Comp. Mater. Sci.*, 2006, **36**, 354-360.

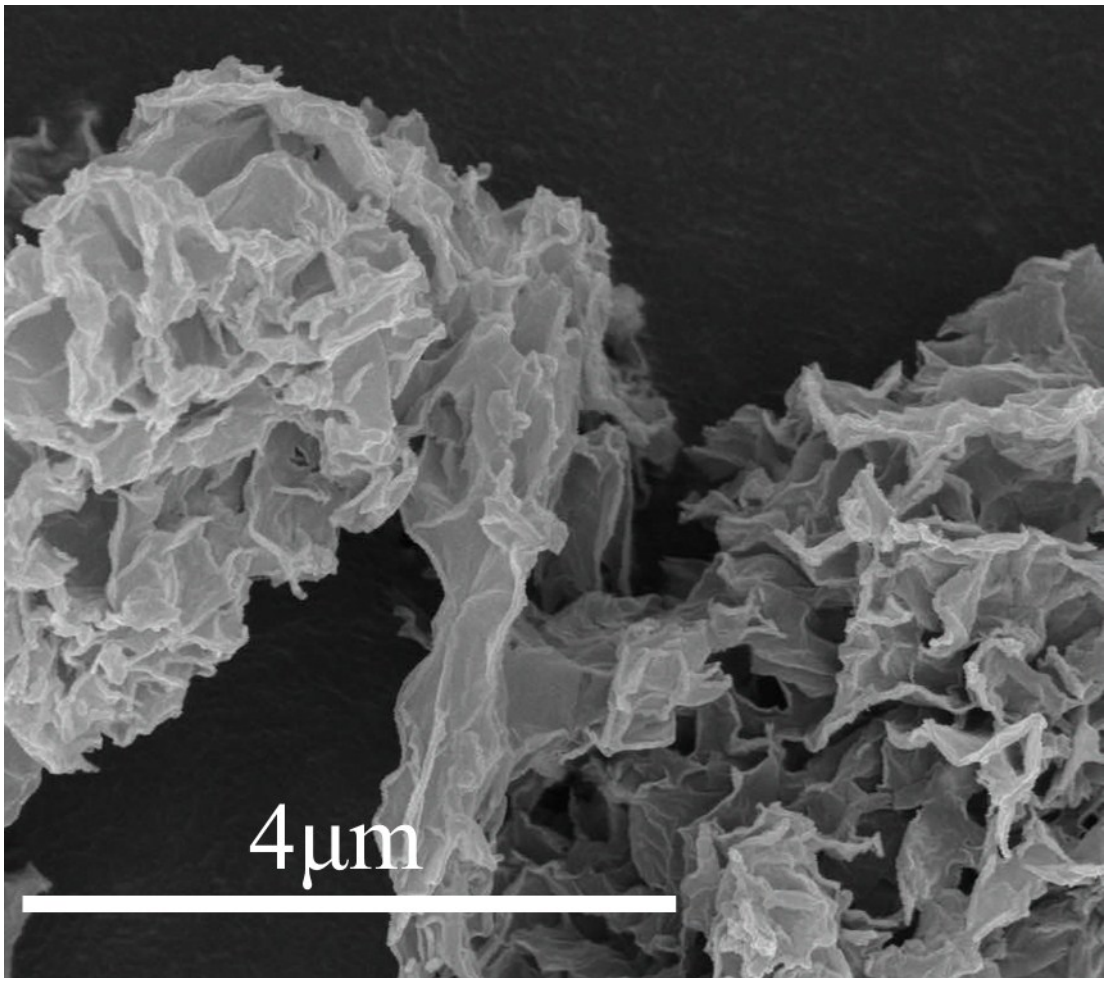

Figure. S1. SEM image of the 3DNG.

The 3DNG has surface area of 548.7 m2 g^{-1} and total pore volume of 1.76 cm3 g^{-1} as reported before. (*Adv. Mater.* **27,** 5171–5175 (2015))

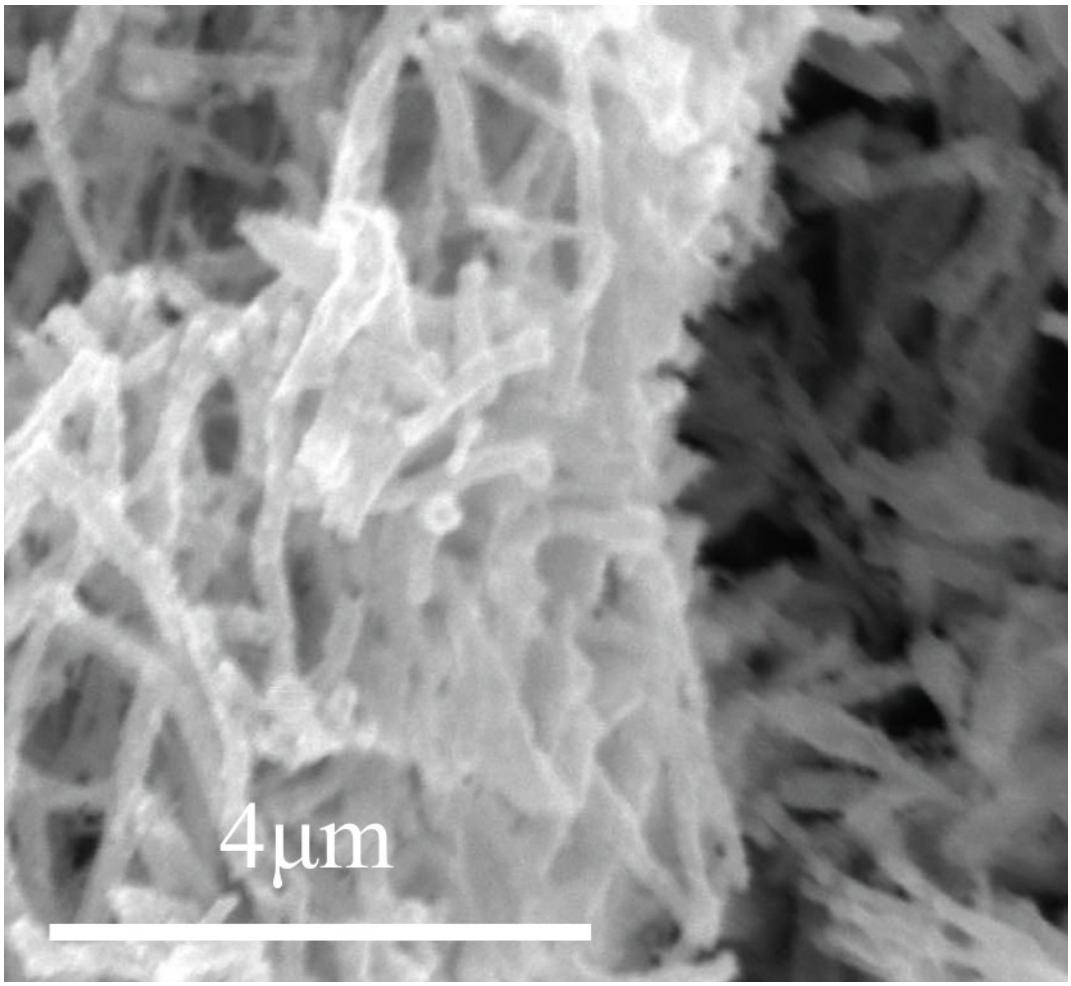

Figure. S2. SEM image of the P-HF.

The PBSCF precursor nanofiber would break and shrinking into a hollow nanofiber with an average diameter of ~200 nm. All the P-HF showed consistent diameter size and same morphology due to the optimization of the ramping rate, calcination temperature and the quality of precursors.

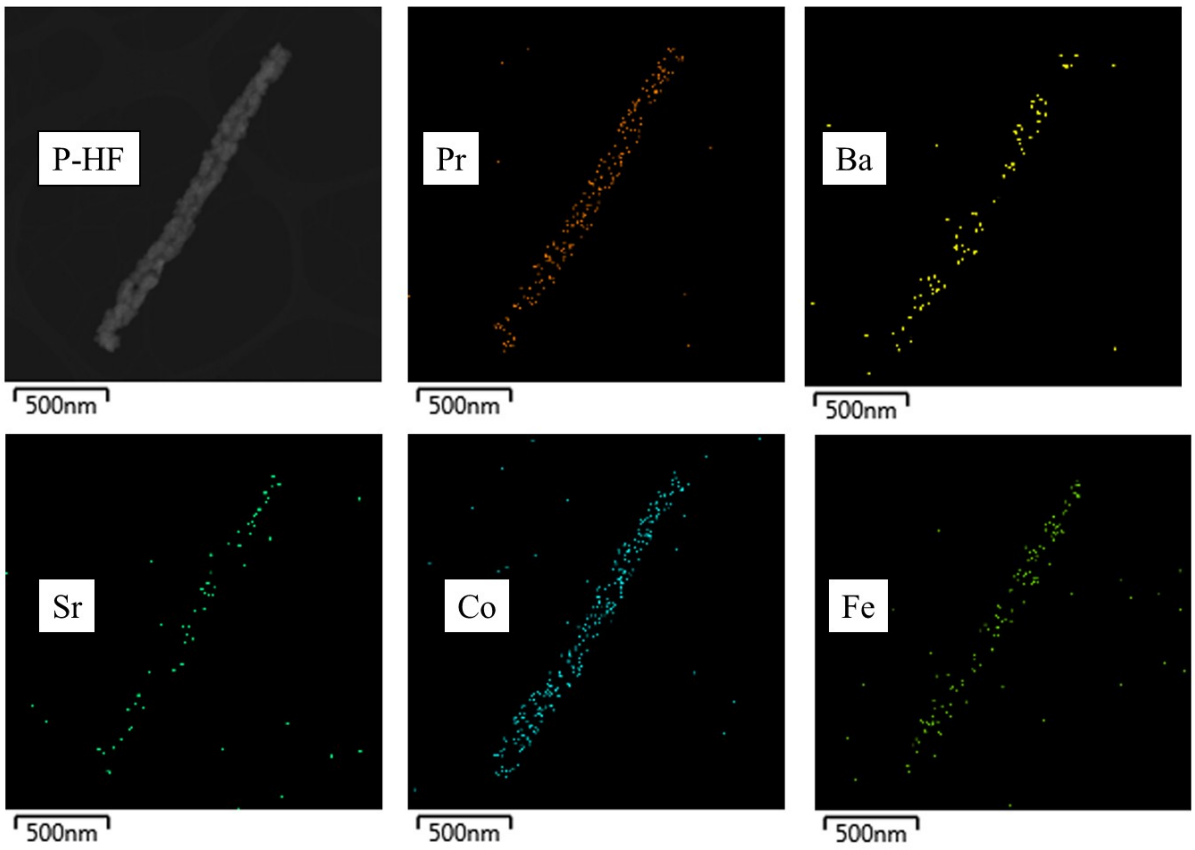

Figure. S3. STEM and corresponding EDX element mapping image of the P-HF.

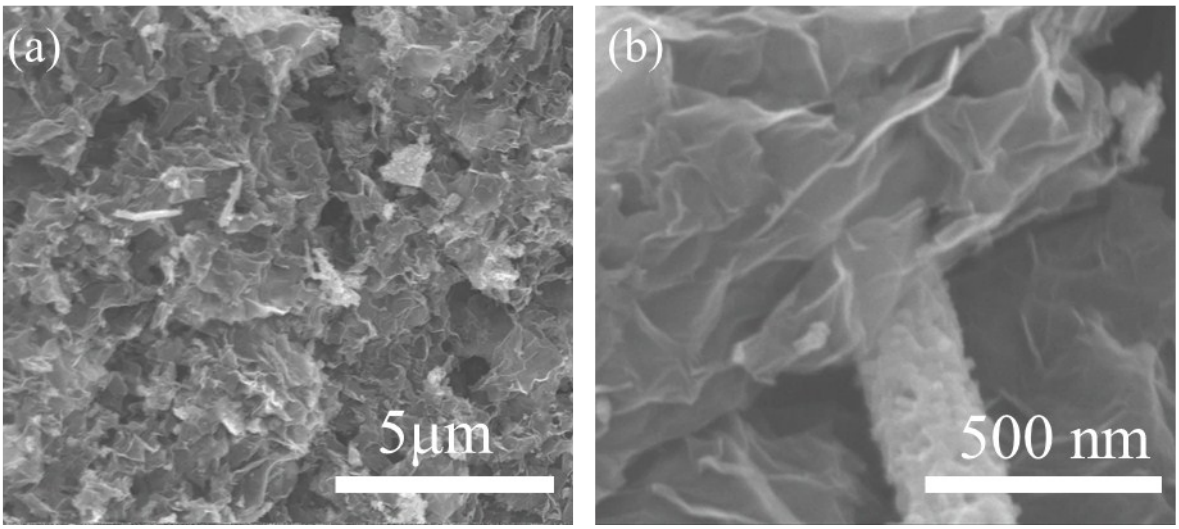

Figure. S4. SEM image of the P-3G.

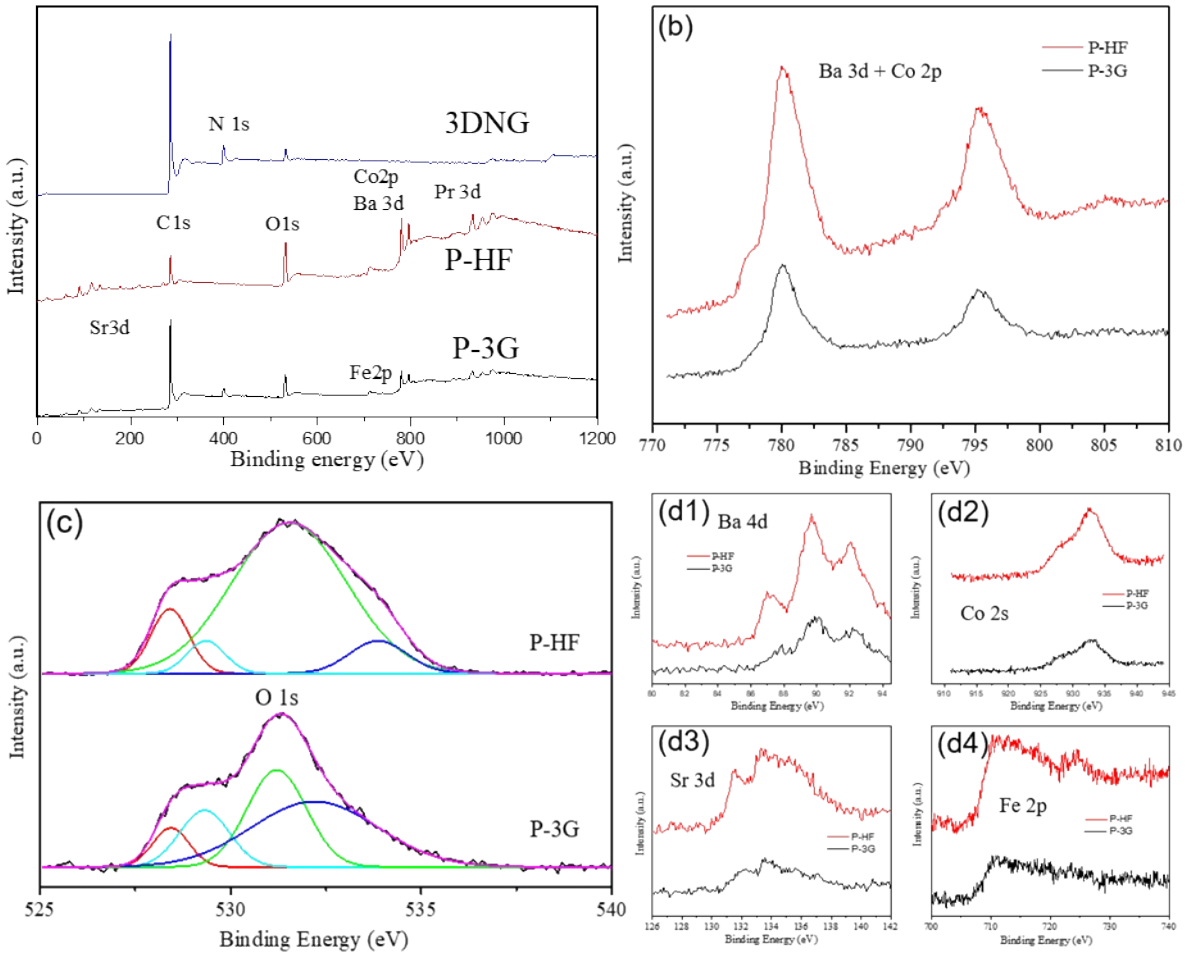

Figure. S5. XPS data of the P-HF and P-3G.

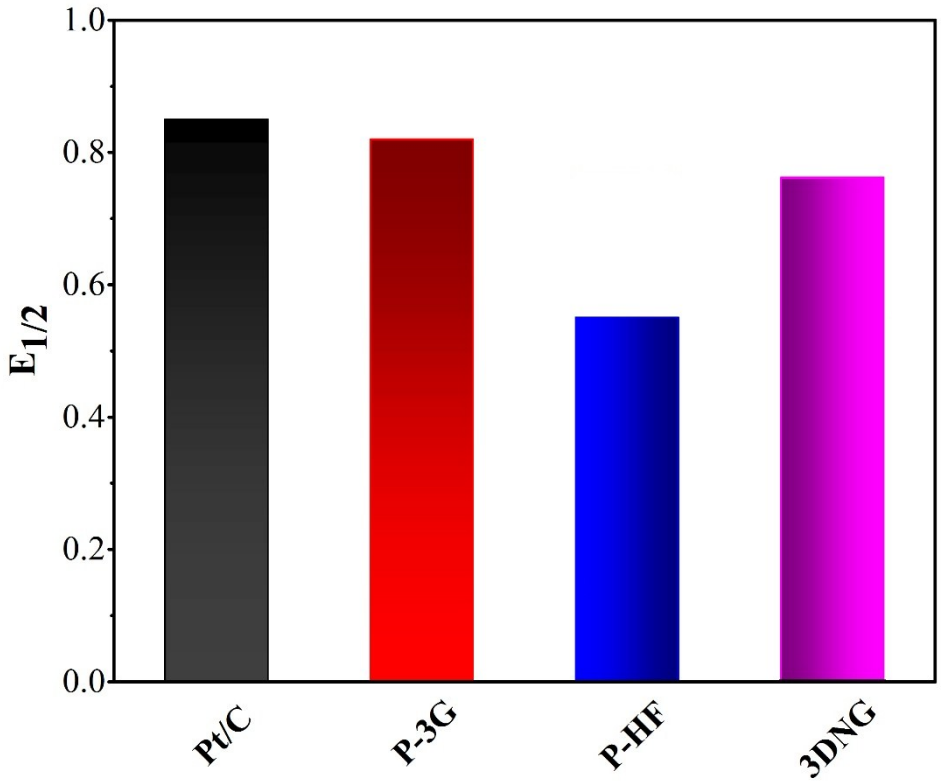

Figure. S6. Half-wave potential ($E_{1/2}$) of the P-3G, Pt/C, 3DNG, and p-HF at current density of 10 mA cm^{-2}.

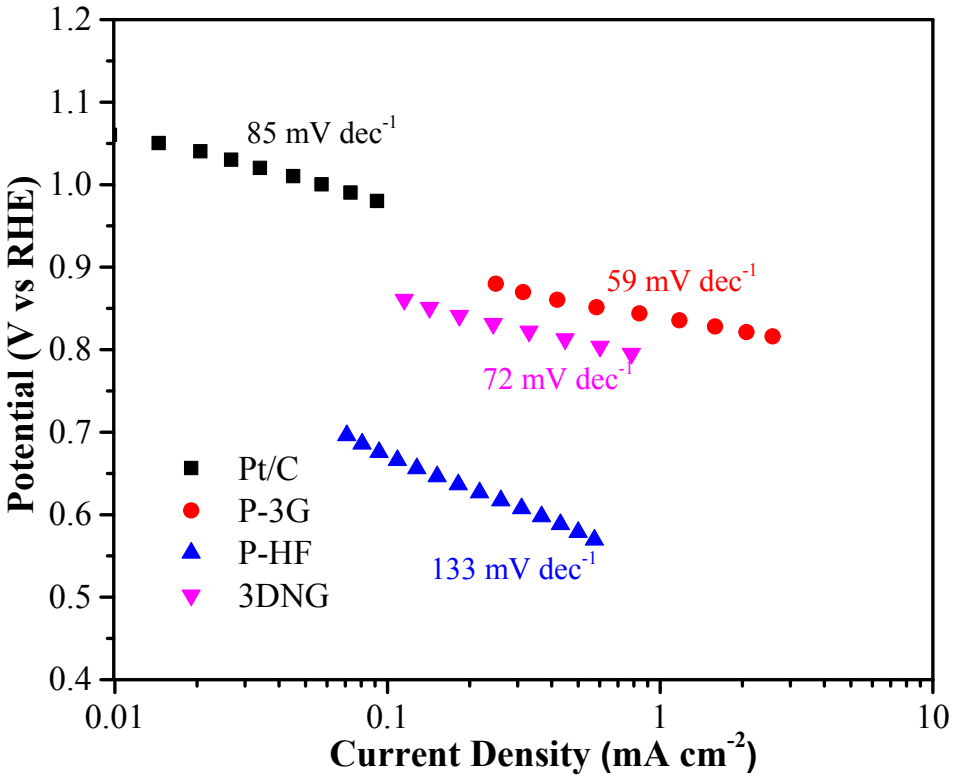

Figure. S7. Tafel plots obtained from the polarization curves in polarization curves of the P-3G, P-HF, Pt/C and 3DNG electrocatalysts in 0.1 M KOH solution.

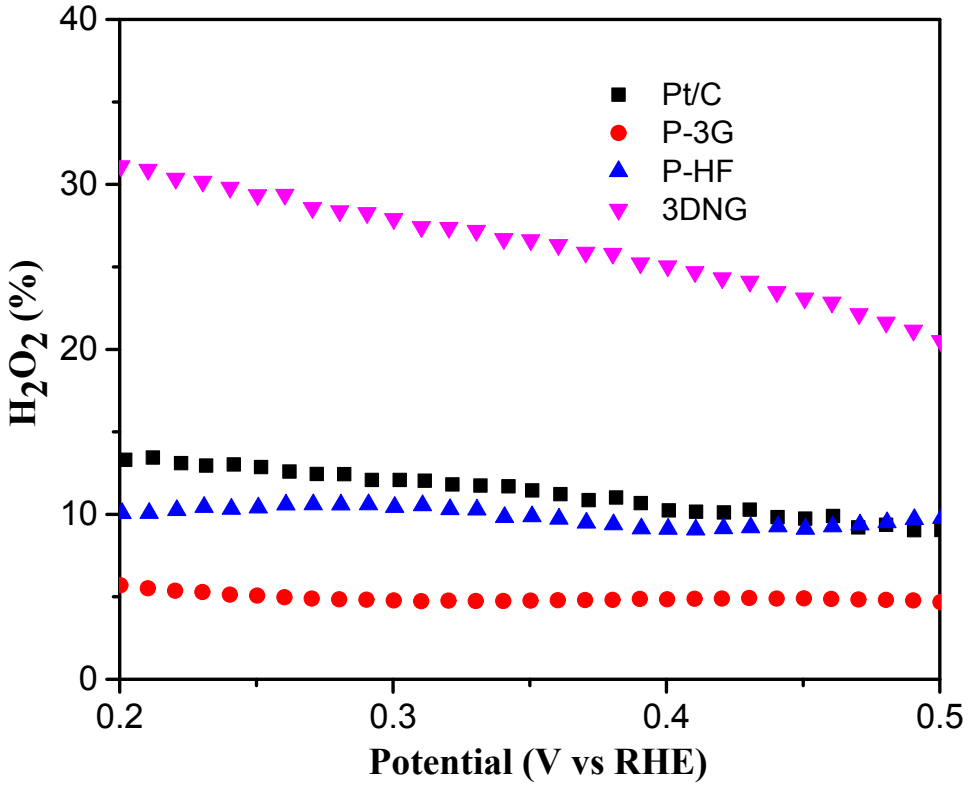

Figure. S8. H_2O_2 yields of the P-3G, Pt/C, P-HF and 3DNG.

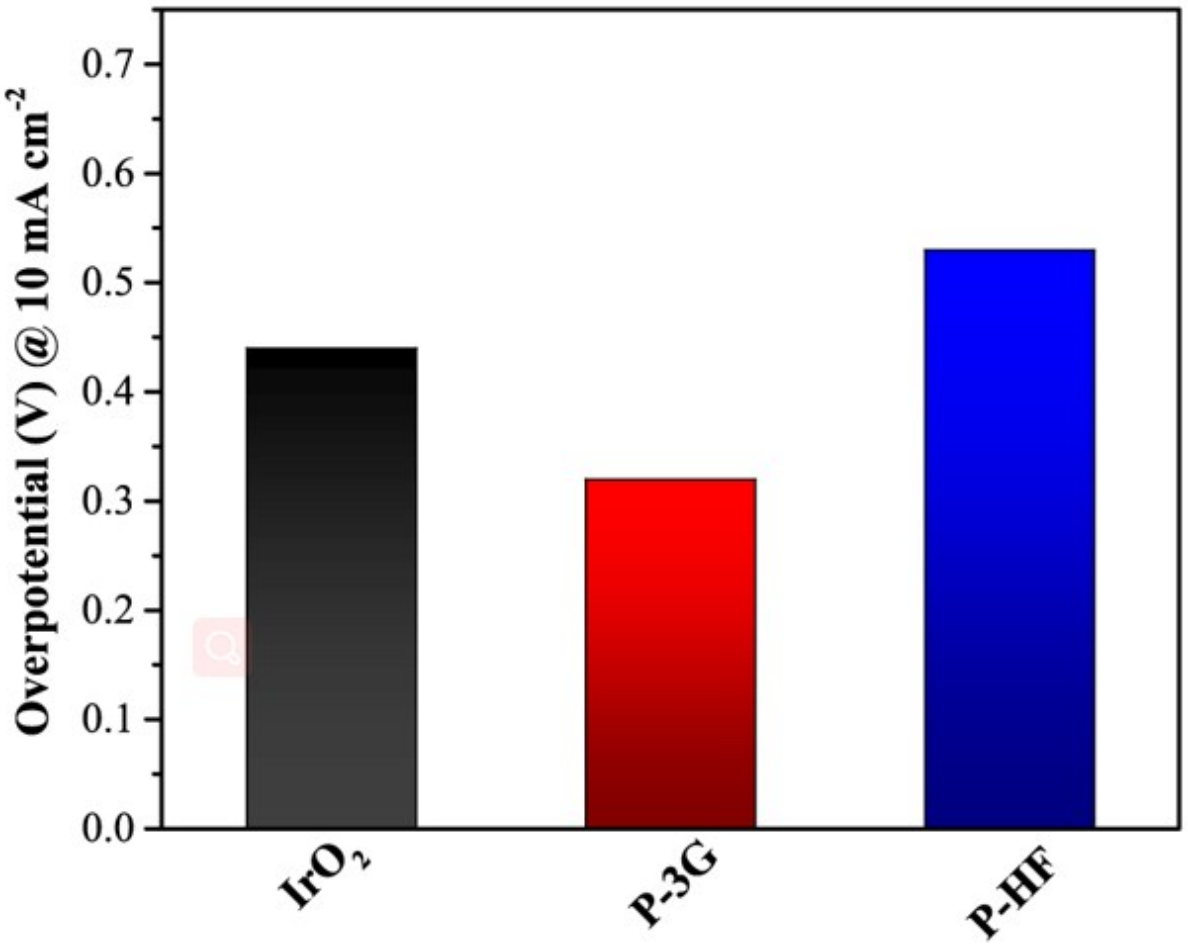

Figure. S9. Overpotentials of the P-3G, P-HF, and IrO_2 at current density of 10 mA cm^{-2}.

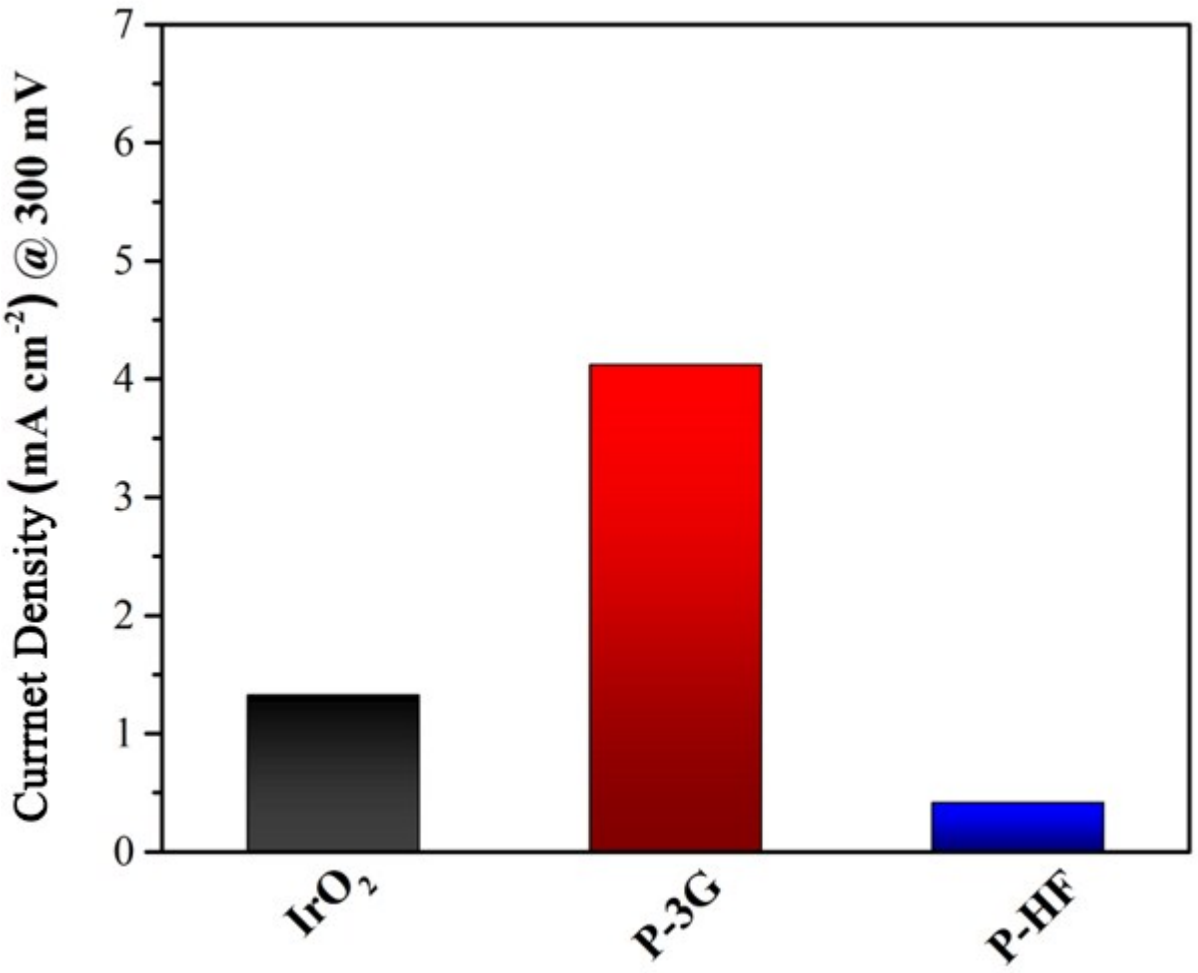

Figure. S10. Currents densities of the P-3G, P-HF, and IrO_2 at overpotential of 0.32 V.

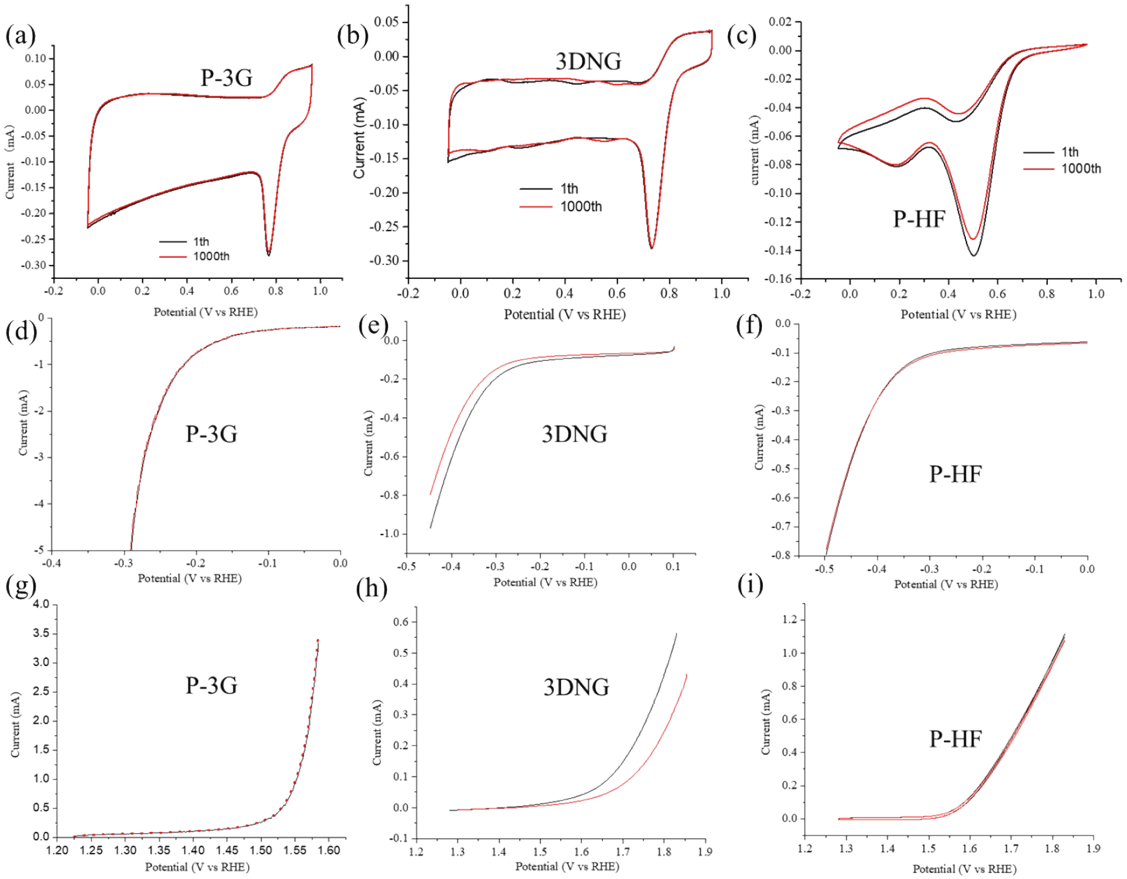

Figure. S11. Durability test of the P-3G，3DNG, and P-HF.

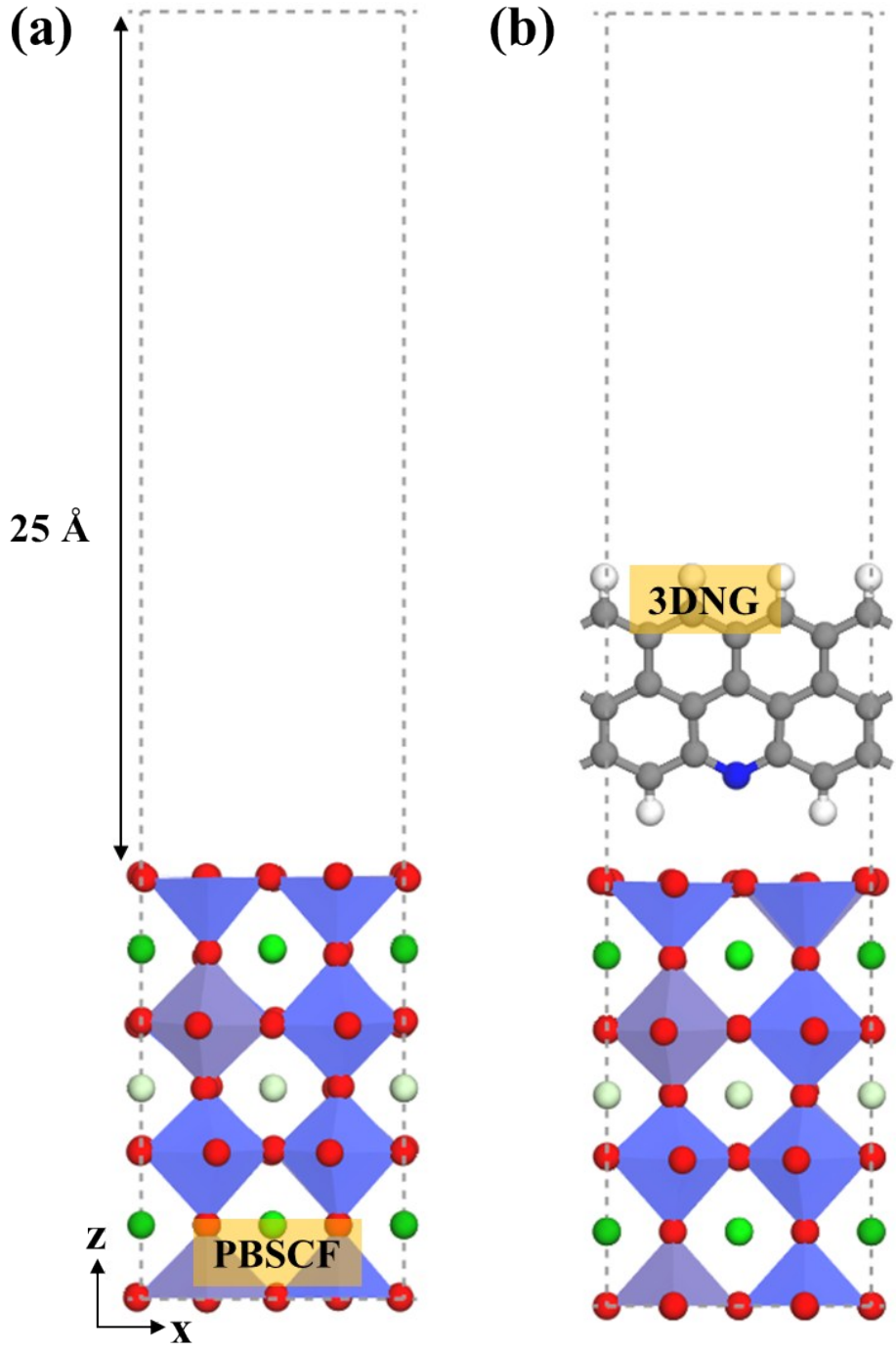

Figure. S12. A symmetric slab model of (001) surface consisting of 7 atomic layers was constructed with the vacuum slab of 25 Å to avoid interaction between adjacent periodic slabs along the *z*-axis of PBSCF and 3DNG.

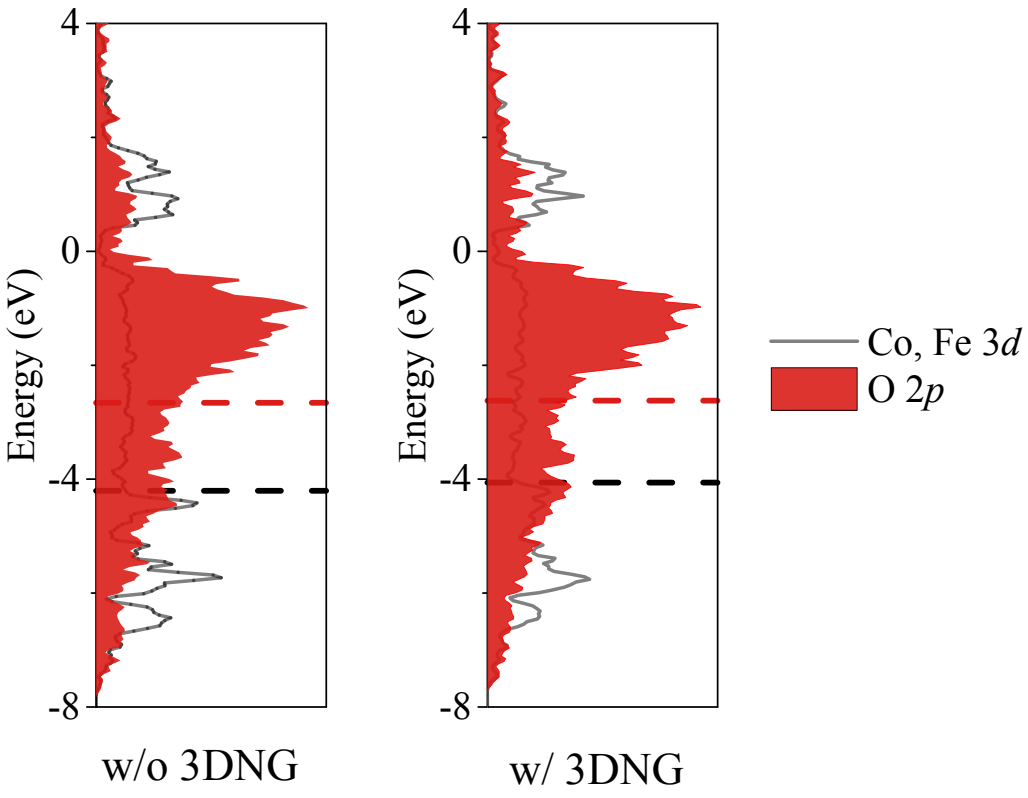

Figure. S13. Projected density of states (PDOS) for Co, Fe 3*d*-orbitals and O2*p*-orbitals of PBSCF without and with 3DNG. Black and red dashed line indicates 3*d*- and 2*p*-band center, respectively.

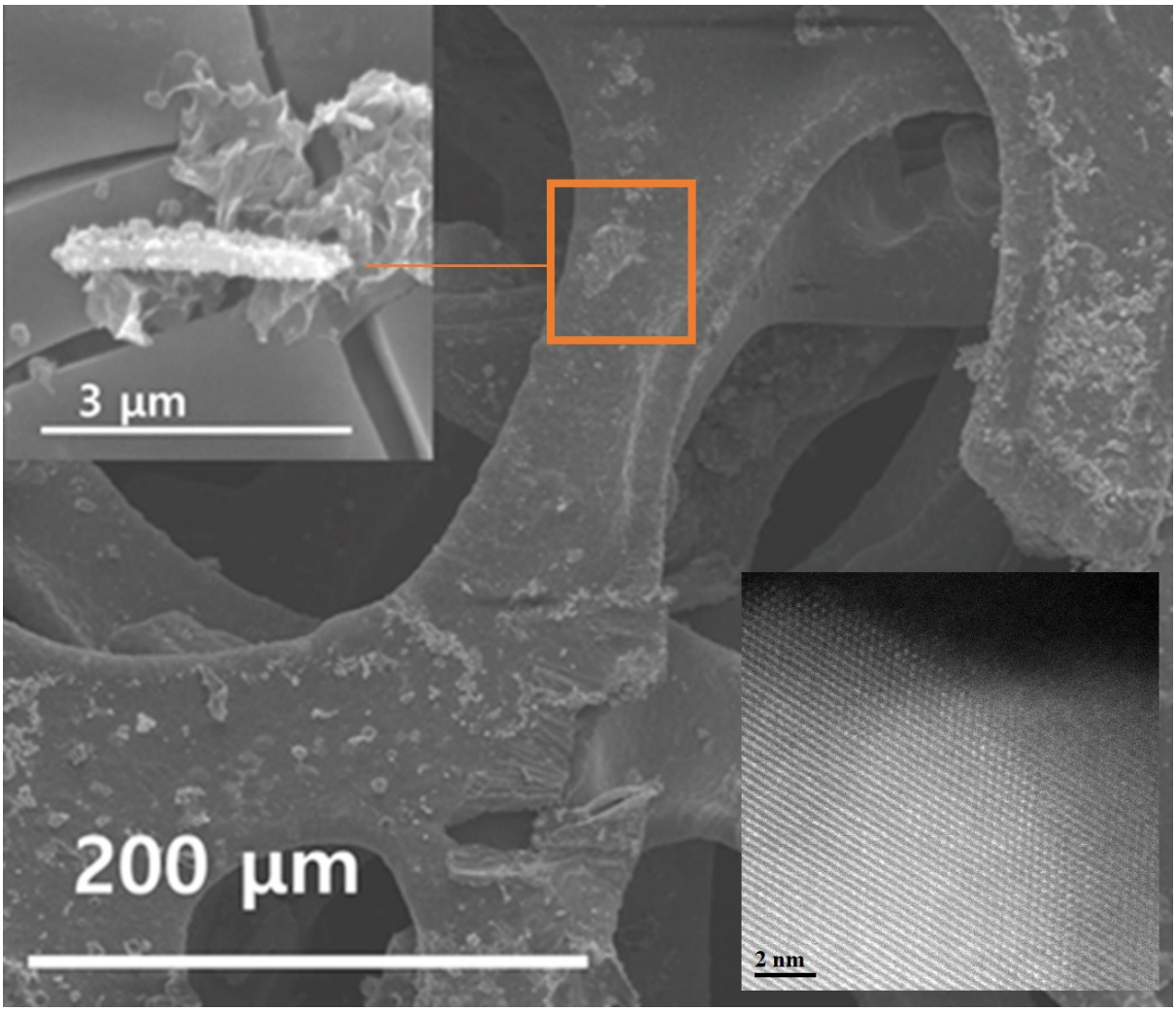

Figure. S14. The TEM and HR-TEM picture after the Zn-air battery long stability test.

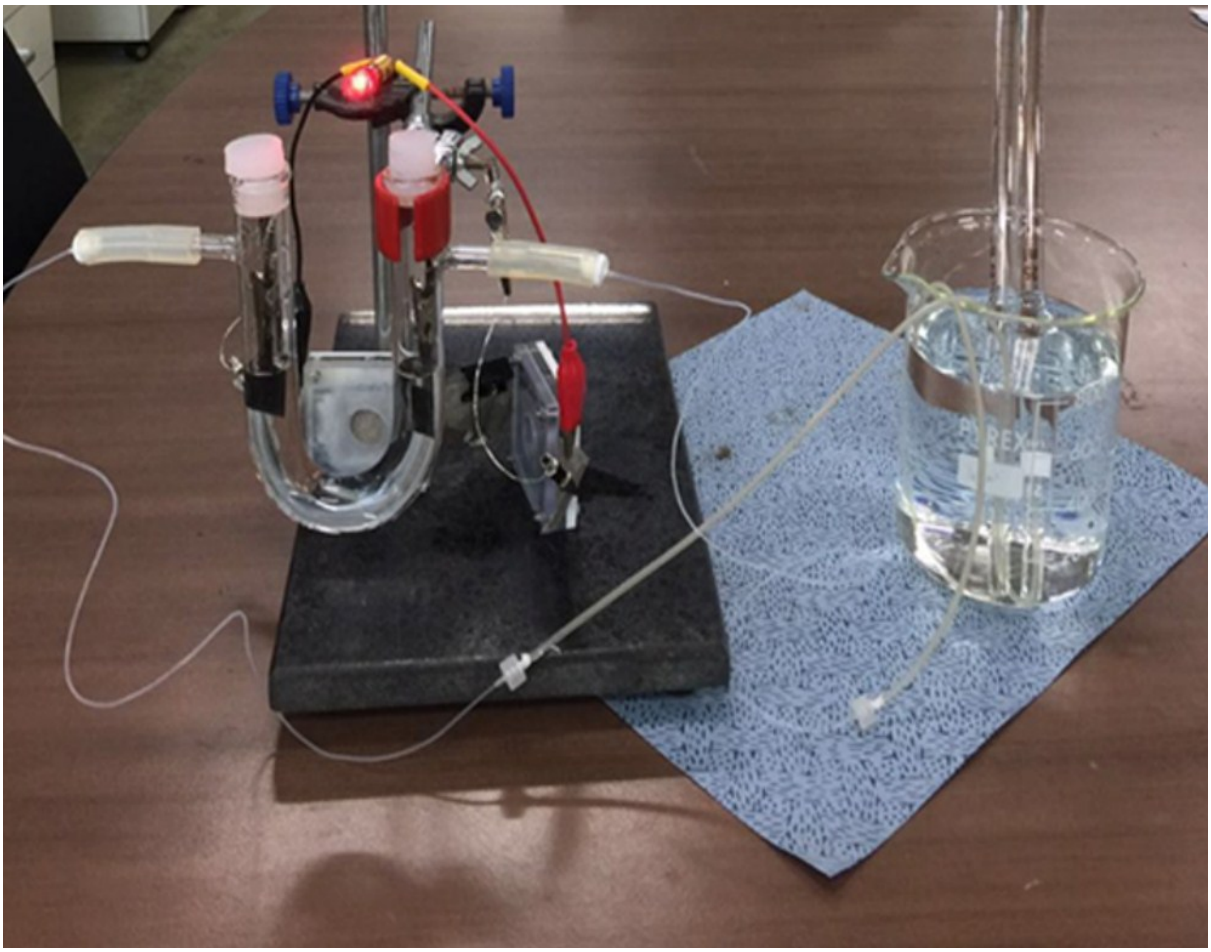

Figure. S15. Digital image of the water electrolysis.

The generated H_2 and O_2 from different sides of the sealed U-type tube were bubbled into tubes with volume marks under water respectively. Then, the produced H_2 and O_2 volume were recorded by the tube water surface level dropped down with increasing water-splitting time.

Table. S1. Comparison of the ORR performance of the P-3G with reported other reported metal oxides electrocatalysts in alkaline solution.

Catalysts	$E_{1/2}$ (V vs.RHE)	Onset potentials (V vs. RHE)	Electron transfer number (n) @ 0.6 V	Tafel slope (mV dec^{-1})	References
P-3G	0.82	0.89	3.81	59	This work
$La_{0.7}(Ba_{0.5}Sr_{0.5})_{0.3}Co_{0.8}Fe_{0.2}O_{3-\delta}$	~0.76	0.72	-	>120	*Energy Environ. Sci. 2016, 9, 176*
$Co_{0.5}0Mo_{0.5}O_yN_z$ / C	0.76	0.92	3.85	71	*Angew Chem Int Edit. 2013, 52(41), 10753*
Fe−N/C−800	0.81	0.92	3.96	-	*J Am Chem Soc. 2014, 136(31): 11027*
N-CG–CoO	0.81	0.90	4.0	48	*Energy Environ Sci. 2014, 7(2): 609*
Co_3O_4–NrmGO	0.83	-	3.9	42	*Nat Mater. 2011, 10(10): 780*
Fe_3C/C-800	0.83	1.05	-	59	*Angew Chem Int Edit 2014, 53(14): 3675*
NCNT/CoO-NiO-NiCo	0.83	1.0	3.9	63	*Adv. Funct. Mater. 2015, 25: 5799*
CoO/NCNT	0.86	0.93	3.9	-	*J Am Chem Soc. 2012, 134(38): 15849*
Fe−N_4/C	0.87	-	-	55	*J Am Chem Soc. 2013, 135(41): 15443*
$Co_{1-x}S$/RGO	-	0.87	4	-	*Angew Chem Int Edit. 2011, 50(46): 10969*
$LaTi_{0.65}Fe_{0.35}O_{3-\delta}$ @ Nitrogen doped carbon nanorods	-	0.78	4	84	*Nano Energy. 2015, 15, 92*

Table. S2. Summary of some recently reported representative OER electrocatalysts in alkaline solution.

Catalysts	η @ 10 mA cm^{-2} (mV)	Tafel slope (mV dec^{-1})	References
P-3G	320	74	This work
IrO_2	338	47	*Nature Comm.* ***2014****, 5, 4477*
$(Pr_{0.5}Ba_{0.5})CoO_{3-\delta}$	~340	-	*Nat. Commun.* **2013**, 4, 2439
LCF0.2	340	50	*Adv. Mater.* **2015**, 27, 7150
$NiFeO_x$	350	-	*J. Am. Chem. Soc.* ***2013****,135,16977*
$Ni_{0.25}Co_{0.75}O_x$	377	36	*J. Am. Chem. Soc.* ***2012****, 134, 17253*
$Au@Co_3O_4$	380	60	*Adv. Mater.* **2014**, 26, 3950
SNCF-NR	389	61	*Adv. Energy Mater.* ***2016****, 1602122*
LT-$Li_{0.5}CoO_2$	~390	60	*Nat. Commun.*, **2014**, 5, 3949
RuO_2	390	-	*J. Am. Chem. Soc.* ***2014****, 136(19): 7077*
Co-CoO/N-rGO	~400	68	*Adv. Funct. Mater.* **2015**, 25, 5799
$LiNi_{0.8}Al_{0.2}O_2$	~410	44	*Adv. Mater.* **2015**, 27, 6063
Co_xO_y/NC	430	75	*Angew. Chem. Int. Ed.* **2014**, 53, 8508
$Mn_3O_4/CoSe_2$	450	49	*J. Am. Chem. Soc.* **2012**, 134, 2930
$Ca_2Mn_2O_5$	>470	149	*J. Am. Chem. Soc.* **2014**, *136*, 14646
$SrCo_{0.95}P_{0.05}O_3$	480	84	Adv. Funct. Mater. **2016**, 26, 5862
α-MnO_2-SF	490	78	*J. Am. Chem. Soc.* **2014**, 136, 11452
Zn-Co-LDH	~520	-	*J. Am. Chem. Soc.* **2013**, 135, 17242
NG-CNT	520	141	*Adv. Mater.* **2014**, 26, 2925.
Cu-N-C/graphene	>770	-	*Nat. Commun.* **2014**, 5, 5285.

Table. S3. Summary of some recently reported representative HER electrocatalysts in alkaline solution.

Catalysts	η @ 10 mA cm^{-2} (mV)	Tafel slope (mV dec^{-1})	References
P-3G	229	124	This work
Ni@NC	190	-	*Adv. Energy Mater.* **2015**, 5, 1401660
$Co(OH)_2$	200	-	*Angew Chem Int Edit.* ***2012****, 51(51): 12703*
CoP	210	129	*J Am Chem Soc.* ***2014****, 136(21): 7587*
CoP nanoparticle	~220	-	*ACS Catal*. **2015**, 5, 4066
MoB	225	59	*Angew. Chem. Int. Ed.* **2012**, 51, 12703
Co-PCNFs	249	92	*J. Mater. Chem. A* **2016**, 4, 12818
Fe-WCN	250	-	*Angew. Chem. Int. Ed.* **2013**, 52, 13638.
Ni-NiO/N-rGO	260	67	*Adv. Funct. Mater. 2015, 25: 5799*
SNCF-NR	262	134	*Adv. Energy Mater.* ***2016****, 1602122*
$Co_{0.6}Mo_{1.4}N_2$	~280	-	*J. Am. Chem. Soc,* **2013**, 135, 19186.
$Ni/Ni(OH)_2$	>300	128	*Angew. Chem. Int. Ed.* **2012**, 51, 12495
Mn_1N_1	360	-	*Adv. Funct. Mater.* **2015**, 25, 393
MPSA/GO-1000	~450	-	*Angew. Chem. Int. Ed.*, **2016**, 55, 223
N,P-graphene-1	~610	145	*ACS Nano* **2014**, 8, 5290
C_3N_4@NG	>600	-	*Nat. Commun.,* **2014**, 5, 3783

Table S4. Summary of overall water splitting performance in alkaline solution of some recently well-developed bifunctional non-noble electrocatalysts.

Catalysts	Substrate	$E_{J=10}$[b] (V)	Durability (h)	References
P-3G	Carbon paper	1.71	30	This work
Porous MoO_2	Ni foam	1.53	24	*Adv. Mater.* **2016**, 28, 3785
Ni-P	Carbon fiber paper	1.63	100	*Adv. Funct. Mater.* **2016**, 26, 4067
Ni_2P nanoparticle	Ni foam	1.63	10	*Energy Environ. Sci.* **2015**, 8, 2347
$NiCo_2S_4$ nanowire	Ni foam	1.63	50	*Adv. Funct. Mater.* **2016**, 26, 4661
ONPPGC/OCC	Oxidized carbon cloth	1.66	10	*Energy Environ. Sci.* **2016**, 9, 1210
NiFe/$NiCo_2O_4$	Ni foam	1.67	10	*Adv. Funct. Mater.*, **2016**, 26, 3515
$NiCo_2O_4$ nanowire	Carbon cloth	1.68	10	*Nanoscale* **2015**, 7, 15122
SNCF-NR	Ni foam	1.68	30	*Adv. Energy Mater.* ***2016***, *1602122*
Fe-P nanotube	Carbon cloth	1.69	14	*Chem. Eur. J.* **2015**, 21, 18062
CoP/rGO	Carbon fiber paper	1.70	-	*Chem. Sci.* **2016**, 7, 1690
Co-S sheet	Carbon paper	~1.74	~2	*ACS Nano* **2016**, 10, 2342
Co_3O_4 nanocrystals	Carbon fiber paper	1.91	-	*Chem. Commun.* **2015**, 51, 8066

Table S5. Summary of overall zinc air battery performance of some recently well-developed bifunctional non-noble electrocatalysts.

Catalysts	Electrolytes	Voltage polarization(V) *@ 20 mA cm^{-2}*	Cyclability	References
P-3G	6 M KOH	0.63V	20 mA cm^{-2} 600 s per step 110 cycles	This work
$CoMn_2O_4$/N-rGO	6 M KOH	~0.7 V	~ 8 mA cm^{-2} 300 s per step 50 cycles	*Electrochim. Acta*, **2012**, 69, 295
$NiCo_2O_4$	6 M KOH	~0.7 V	15 mA cm^{-2} 7 min per step 60 cycles	*Nanoscale*, **2013**, 5, 4657
La_2NiO_4	6 M KOH	~0.8 V	20 mA cm^{-2} 300 s per step 100 cycles	*Electrochem. Commun.*, **2014**, 41, 59
$LaNiO_3$/NCNT	6 M KOH	~1.2 V	20 mA cm^{-2} 20 min per step 50 cycles	*Nanoscale*, **2014**, 6, 3173
MnO_2/Co_3O_4	6 M KOH	~1.4 V	~17.6 mA cm^{-2} 300 s per step 75 cycles	*Nano Lett.*, **2012**, 12, 1946
MnO_2–NCNT	6 M KOH	~1.5 V	~25 mA cm^{-2} 150 s per step 20 cycles	*ACS Appl. Mater. Interfaces*, **2013**, 5, 9902